NACA

RESEARCH MEMORANDUM

INFLUENCE OF A CANARD-TYPE CONTROL SURFACE ON THE INTERNAL AND EXTERNAL PERFORMANCE CHARACTERISTICS OF NACELLE-MOUNTED SUPERSONIC DIFFUSERS (CONICAL CENTERBODY) AT A REARWARD BODY STATION FOR A MACH NUMBER OF 2.0

By L. J. Obery and H. S. Krasnow

Lewis Flight Propulsion Laboratory
Cleveland, Ohio

NATIONAL ADVISORY COMMITTEE
FOR AERONAUTICS
WASHINGTON
August 12, 1952

NATIONAL ADVISORY COMMITTEE FOR AERONAUTICS

RESEARCH MEMORANDUM

INFLUENCE OF A CANARD-TYPE CONTROL SURFACE ON THE INTERNAL AND EXTERNAL PERFORMANCE CHARACTERISTICS OF NACELLE-MOUNTED SUPERSONIC DIFFUSERS (CONICAL CENTERBODY) AT A REARWARD BODY STATION FOR A MACH NUMBER OF 2.0

By L. J. Obery and H. S. Krasnow

SUMMARY

The effects of the wake resulting from control-surface deflection on the internal performance of two supersonic diffusers (conical centerbody type) and on the engine-body interference drag were investigated in the Lewis 8- by 6-foot supersonic wind tunnel at a Mach number of 2.0, angles of attack from 0° to 10°, control-surface deflection angles from 0° to $9\frac{1}{2}^\circ$, and at a Reynolds number of approximately 1.5×10^6 based on inlet diameter. Nacelle-type engines were mounted on a body of revolution approximately 10 mean chords downstream of and in the plane of the control surface. The diffuser performance was determined at two spanwise locations: (1) alined with, and (2) approximately 6 inches outboard of the control-surface tips. A modified diffuser was investigated in the outboard location. Both diffusers were tested in the undisturbed stream.

The investigation indicated that severe performance penalties result if the inlet is immersed in the disturbed flow resulting from the trailing vortex, but that these penalties may be considerably mitigated by a rather small outboard shift of the engines. At the higher angles of attack and with the control surface removed, the upwash field generated by the body increased the angle-of-attack effects of the diffuser by approximately 40 percent for both engine locations.

For the inboard engine location, the favorable interference drag produced by the relative location of the engines and the body was not affected by control-surface deflection.

INTRODUCTION

A serious problem in the design of a missile is the arrangement of the component parts of the configuration. Although the characteristics of each part may be calculated or obtained experimentally, the over-all performance of the missile will depend upon the interrelation of the components and the interaction of one component on another.

Recent investigations (references 1 and 2) have shown that a favorable interference drag can be produced from the relative location of the missile components, that is, the drag of the complete missile is less than the sum of the individual drags. For a fuselage with nacelle engines, the drag will be a minimum when the engines are located close to the body and at a station downstream of the maximum diameter of the body (reference 1). For a fuselage-nacelle engine configuration of this type, a canard-type control surface may be advantageous. With lift, however, a rolled-up vortex sheet is generated by the control surface, the effects of which appear as losses in total pressure and as flow angularity. These effects spread laterally as the vortex moves downstream and if the air inlet is located in this disturbed air-flow region, serious performance penalties can result which may, in turn, alter the selection of component arrangements.

This investigation was conducted to determine the effects of the wake resulting from control-surface deflection on the performance of two different diffuser designs mounted on a typical missile configuration and to indicate to what extent the control might influence the missile arrangement. The investigation was conducted in the NACA Lewis 8- by 6-foot supersonic wind tunnel at a Mach number of 2.0, angles of attack from 0° to 10°, control-surface deflections from 0° to $9\frac{1}{2}^\circ$, and a Reynolds number of approximately 41×10^7 based on body length.

SYMBOLS

The following symbols are used in this report:

A_c	control-surface plan area, including area formed by extending leading and trailing edges to body center line, 0.937 sq ft
A_f	frontal area of body, 0.442 sq ft
C_D	drag coefficient, D/q_0A_f
D	drag
M_0	free-stream Mach number

m_2/m_0 mass-flow ratio, value of 1 when free-stream tube, as defined by cowl lip, enters engine

P total pressure

p static pressure

q_0 free-stream dynamic pressure, $\gamma p_0 M_0^2/2$

α angle of attack

δ control-surface deflection away from body center line, positive deflection same sense as positive angle of attack

Subscripts:

0 free stream

2 station in subsonic diffuser

3 entrance to engine combustion chamber

A conditions in flow field immediately ahead of diffuser

l local

max maximum

APPARATUS AND PROCEDURE

The model used in this investigation (fig. 1) consisted of a body of revolution with a canard-type control surface and two nacelle engines mounted in the horizontal plane. The body had a length-diameter ratio of 12 and a maximum diameter of 9 inches.

The control surface used with the inboard engine location had a plan area A_c of 0.937 square feet, an aspect ratio of 3.0, a taper ratio of 0.5, and an unswept 50-percent chord line. The airfoil section was a double circular arc, 5-percent thick except near the root where the thickness was increased to 8 percent for structural reasons. The all-movable control surface was hinged about its 50-percent chord line and was remotely operated. The nose portion of the body adjacent to the forward half of the control was fixed to and deflected with the surface.

Two diffusers (fig. 2) were investigated. The first (fig. 2(a)) was designed with a straight-taper cowl of low divergence in order to obtain minimum drag, and for the second (fig. 2(b)), the low drag

characteristics were compromised in favor of higher pressure recovery by employing a high-angle lip and a constant-area section for boundary-layer stabilization. This inlet also had four removable cowl struts located 90° apart to simulate structural struts that might be used on a full scale engine. The coordinates for the second diffuser are presented in figure 2. Neither diffuser utilized internal contraction.

The engines were mounted in two lateral locations, $1\frac{1}{2}$ and 2 engine diameters from the fuselage, designated herein as inboard-engine location and outboard-engine location, respectively. The straight-taper diffuser was tested in both locations and alone in the undisturbed stream. The second diffuser was tested only in the outboard location and in the undisturbed stream.

The inlets were nearly alined with the tips of the control surface at zero angle of attack for the inboard-engine location. For the investigation with the engine in the outboard location, the span of the control was reduced by approximately 6 inches, thus placing each engine about 6 inches outboard of the control tips without using excessively long support struts.

Also shown in figure 2 is the orifice used to control engine mass flow. The orifice consisted of two circular flat plates with open area segments. The open area was varied by rotating one of the plates with respect to the other. Previous calibration had determined that for the range of flow conditions in the engines the orifice-plate flow coefficient was approximately 0.87.

Instrumentation for all engines included static-pressure measurements at stations 3 and B. For one of the diffusers in the inboard location and for the modified diffuser, total- and static-pressure rakes were located at station 2. In addition, total-pressure tubes were flush mounted in the inlet cowl struts (station 1) of the modified engine.

The mass flow through the engines was determined from the known open area at the orifice and the static pressure measured at station B with the assumption that the exit area was choked. The mass flow is believed accurate to ±3 percent. Total-pressure recovery P_3/P_0 was determined from the known mass flow and the static pressure measured at station 3 and is considered accurate to ±1 percent.

DISCUSSION

Internal-Flow Evaluation

Straight-taper-cowl diffuser. - In order to determine a basis for comparison of the internal performance of the several model configurations, the straight-taper diffuser was tested alone in the undisturbed stream. The diffuser performance is shown in figure 3, where the total-pressure recovery is presented as a function of mass-flow ratio. Total-pressure recovery is defined as the total pressure computed at the combustion-chamber inlet divided by free-stream total pressure; and mass-flow ratio is defined as the ratio of the mass flowing through the engine to the mass flowing in a free-stream tube of a diameter equal to that of the engine inlet. From the curves (fig. 3), it is evident that the pressure recovery, the maximum mass-flow ratio, and the stable subcritical range decrease considerably as the angle of attack is increased. The maximum pressure recovery measured in this diffuser was quite low (81 percent). This low recovery probably resulted from the low cowl-lip angle which produced an abrupt change in the flow direction at the lip and (because the diffuser had no constant-area section for boundary-layer stabilization) probably adversely influenced the boundary layer on the cowl walls. This presumption was supported by total-pressure data at station 2 (not included in this report), which indicated that the low-energy air was located in an annular area at the cowl walls. The straight-taper cowling also caused an abrupt change in curvature of the centerbody (fig. 2(a)) to avoid internal contraction which probably also adversely affected the diffuser performance.

Locating the engine near the body ($1\frac{1}{2}$ engine diameters from the body center line, fig. 1), had a negligible effect on the pressure recovery but reduced the mass flow approximately 1 percent at the lower angles of attack, as shown in figures 4 and 5. However, at angles of attack of 6° and 10°, both the pressure recoveries and the mass-flow ratios were significantly reduced by the presence of the body. The range of stable subcritical operation (fig. 4), however, was essentially the same as for the investigation of the engine alone. The adverse effects at the higher angles of attack, as compared with engine-alone performance, are due to the upwash field generated by the body. Flow surveys presented in reference 3 show this upwash field and indicate that, at an angle of attack α of 6°, the increased flow angle of attack is approximately $2\frac{1}{2}^\circ$, an increase of about 40 percent. As shown in figure 5, at an α of 10° the maximum pressure recovery of the engine-body combination is approximately the same as for the engine alone at an α of 14°, indicating again that the effective angle of attack is increased by as much as 40 percent by the flow around the body.

The diffuser characteristics for the complete configuration (engines, body, and control surface) are shown in figure 6 for the inboard engine location. With the engines located $1\frac{1}{2}$ engine diameters from the model center line, the inlets were almost alined with the control-surface tips. For an α of 0°, the addition of the control surface at zero deflection decreased the pressure recovery approximately 1 percent of free-stream total pressure and reduced the maximum captured mass flow approximately 3 percent. Since it was shown before that at an α of 0° the body effects were very small, these reductions are due primarily to the reduced available total pressure in the wake, even though the control surface was at an α of 0°. Increasing the control-surface deflection caused a considerable reduction in diffuser performance, especially at a δ of $9\frac{1}{2}^\circ$ where the peak pressure recovery was reduced by more than 12 percent from the value at a δ of 0°.

At an angle of attack of 3°, control deflection resulted in performance reductions similar to those at an α of 0°, except for a δ of $9\frac{1}{2}^\circ$ where the effect was less pronounced. As the angle of attack is increased, the adverse effects of control deflection are reduced because of the vortex core passing above the inlet.

In order to provide some insight into the mechanism whereby the diffuser is affected by the control-surface wake, a flow survey was taken at the inlet station. The results of this survey are presented in reference 3 and are partly reproduced in figure 7 which shows the available total pressure and the flow angularity at the inlet station (the dotted circle represents the inlet). Figure 7 also shows contours of diffuser total-pressure recovery in the annulus at station 2. Figure 7(a) represents the distribution for diffuser operation near critical (marked A in fig. 6) for an α of 0° and a δ of 0°. Because neither the control nor the body were producing lift, no flow angularity was observed although the wake from the control surface was slightly displaced below the model center line. This displacement resulted from a slight pressure gradient developed by the support strut. Part of the wake enters the inlet and produces a significant asymmetric pressure distribution; however, the effect on total-pressure recovery as shown in figure 6(a) is rather small. Figure 7(b) shows the distribution for point B of figure 6, which was the peak-pressure-recovery point for the configuration at an α of 0° and a δ of $9\frac{1}{2}^\circ$. The total-pressure distribution in figure 7(b) indicates that a very low pressure area exists in the entire lower right quadrant. The possibility of separation exists in the region where the total-pressure ratio is below 0.55, because this is approximately equal to wall static pressure. The total-pressure distribution from the flow survey shows that a correspondingly

low total-pressure region exists in this area in the flow field ahead of the inlet. The flow-angularity plot shows rather large deflections all around the inlet; however, the largest deflections are centered about this region of low total pressure, approximately 6° sidewash and $4\frac{1}{2}$° upwash. It thus appears that both low available total-pressure air and flow angularity affect the pressure recovery of the diffuser. Figures 7(c) and 7(d) represent, respectively, data points marked as C and D on figure 6 and show that the regions of low total pressure at station 2 (diffuser total-pressure distributions) correspond, in general, to the regions of low available total pressure at the inlet station. The flow angularities induced by the control surface and the body also undoubtedly affect the distribution; however, no clear trend is apparent for these conditions. At an angle of attack of 10° (point E on fig. 6), however, the diffuser is primarily affected by the flow angularity as shown in figure 7(e). The flow survey shows only a slight available total-pressure loss, whereas, the flow deflections induced by the body, added to the 10° angle of attack of the engine, caused large losses in the diffuser. Thus, apparently both a reduced available total pressure and an increased flow angularity (due either to the control or the body) can cause regions of low total pressure in the diffuser passage. These low-energy regions can be particularly serious in the burning case and certainly would cause added complications to the fuel injection and distribution problem.

The performance characteristics of the straight-taper diffuser for the outboard-engine location configuration are shown in figure 8. With the inlet located well outside the free-stream projection of the control-surface tips, the diffuser performance was not seriously affected by control deflection, although measurable changes were noted. At the higher angles of attack, because control deflection had only a relatively small effect on the pressure recovery and the mass-flow ratio, the large decreases from the engine-alone characteristics can be attributed to the upwash field produced by the body. In figure 9, a comparison of the diffuser performance for the two engine locations shows that, in general, the pressure recovery for the inboard-engine location was lower than the recovery for the outboard-engine location. At the high angles of attack, control deflection had comparable effects on the diffusers for both engine locations, as did body upwash. At the lower angles, however, control deflection had a considerably more adverse effect on the diffuser performance for the inboard-engine location. This suggests that the effects of the vortex developed by the control-surface tips (or the rolling up of the vortex sheet) remains somewhat localized as the vortex moves downstream and that the large reductions in diffuser performance may be considerably mitigated by a rather small outboard shift in the inlet location if a canard-type control is to be used.

High-pressure-recovery diffuser. - The diffuser designed for high pressure recovery was tested in the undisturbed stream and in the outboard-engine location on the body to determine if performance reductions comparable to those of the straight-taper diffuser would result from a high-performance diffuser. The characteristics of this diffuser tested in the undisturbed stream both with and without cowl struts are shown in figure 10. Comparison of the recovery of the modified diffuser with the straight-taper diffuser indicates that the modified design gave much better total-pressure recoveries at all angles of attack up to 16°. Because both conical center bodies were of 25° half-angle, the supersonic losses should be about the same, and hence the increased recovery must have resulted from the subsonic diffuser. As shown in figure 2, the modified design has a much more gradual rate of subsonic diffusion than the first diffuser and has a lip angle more nearly alined with the local flow. Theoretical supersonic losses for a 25°-cone half-angle diffuser at an α of 0° and a Mach number of 2.0 are approximately 10 percent of free-stream total; thus the subsonic losses must have been only about $2\frac{1}{2}$ percent of free-stream total for this diffuser.

At angles of attack of 10° and above, the cowl struts improved the pressure recoveries markedly. For example, at an α of 20°, the addition of the cowl struts increased the recovery by about 5 percent of free-stream total. A possible explanation is that the struts acted as turning vanes and by helping to turn the flow, reduced the losses.

The investigation of the modified diffuser in the outboard-engine location on the complete model showed that deflection of the control surface had very little or no effect on the diffuser performance and complete data are not presented. The maximum recoveries for this configuration, as a function of angle of attack, are presented in figure 11. The increasing difference between the engine-alone recoveries and those for the engine-body - control-surface combination indicate that the upwash field of the body influenced the modified diffuser in much the same manner as it influenced the straight-taper diffuser. Probably because the modified design gave such high performance at zero angle of attack, increasing the angle of attack had a more adverse effect on the recoveries than it did for the straight-taper diffuser.

Drag Evaluation

From the investigation of the diffuser characteristics (inboard-engine location) with control deflection, severe penalties have been shown to result in the form of reduced pressure recovery (and hence reduced thrust) from a canard-type control surface. Because favorable drag interference was the chief determinant of this type of component

arrangement, an investigation was conducted to determine the effect of control deflection on the interference drag for supercritical engine flow. The drag coefficient is defined as the sum of all the drag forces on the external surfaces of the model.

The drag of the configuration (body - control surface and two horizontal engines) increased rapidly with control deflection (fig. 12). In order to determine if this increase were due entirely to the increased drag of the control surface at angle of attack, the drag of the control surface in the presence of the body was experimentally determined from the difference in drag between the body plus control-surface combination and the body alone. The control-surface drag (fig. 12) shows that the change in configuration drag is entirely accounted for by the increase in control-surface drag and thus, within the experimental accuracy, the vortex from the control surface had no effect on the favorable interference drag.

Therefore with the engines placed close to the body, two opposing effects are noted. Because the inlets are immersed in the disturbed flow from the control surface, diffuser total-pressure recovery and, hence, engine thrust will be reduced. However, the relative location of the engines and body produced a favorable interference drag and it is possible that this reduction in drag may be greater than the loss of thrust, thus resulting in a net gain in configuration thrust minus drag.

SUMMARY OF RESULTS

An investigation to determine the effects of control-surface deflection on the internal performance of a diffuser at a Mach number of 2.0 and a Reynolds number of 1.5×10^6 based on inlet diameter was conducted in the Lewis 8- by 6-foot supersonic wind tunnel. The diffuser inlets were located approximately 10 mean geometric chord lengths downstream of the control surface. The straight taper diffuser was investigated in two spanwise locations: (1) alined with, and (2) to approximately 6 inches outboard of the control-surface tips at an angle of attack of 0°. The modified diffuser was investigated in the outboard-engine location.

The following results were obtained:

1. If an air inlet is alined with the control-surface tips, severe losses in pressure recovery and mass-flow recovery can result as compared with the diffuser characteristics in the free stream. These losses are due to a reduced available total pressure and to flow angularity in the stream.

2. Moving the inlets outboard of the vortex field from the control-surface tips (1.6 inlet diameters for this model) considerably improved the diffuser performance at the low angles of attack where the control-surface effects are most pronounced.

3. With the control surface removed, the upwash field produced by the body at the higher angles of attack adversely affected the diffusers in both engine locations to approximately the same extent. The flow deflection produced by the body increased the effective angle of attack of the diffusers by approximately 40 percent.

4. From the investigation of the modified diffuser in the undisturbed stream, it is indicated that the addition of cowl struts in the engine inlet may improve the performance considerably at the higher angle of attack, possibly because of the flow-turning effect of the struts.

5. For the inboard-engine location, the favorable interference drag created by the relative positions of the engines and body was not affected by control-surface deflection.

Lewis Flight Propulsion Laboratory
National Advisory Committee for Aeronautics
Cleveland, Ohio

REFERENCES

1. Kremzier, Emil J., and Dryer, Murray: Aerodynamic Interference Effects on Normal and Axial Force Coefficients of Several Engine-Strut-Body Configurations at Mach Numbers of 1.8 and 2.0. NACA RM E52B21, 1952.

2. Friedman, Morris D.: Arrangement of Bodies of Revolution in Supersonic Flow to Reduce Wave Drag. NACA RM A51I20, 1951.

3. Fradenburgh, Evan A., Obery, Leonard J., and Mello, John F.: Influence of Fuselage and Canard-Type Control Surface on the Flow Field Adjacent to a Rearward Fuselage Station at a Mach Number of 2.0 - Data Presentation. NACA RM E51K05, 1952.

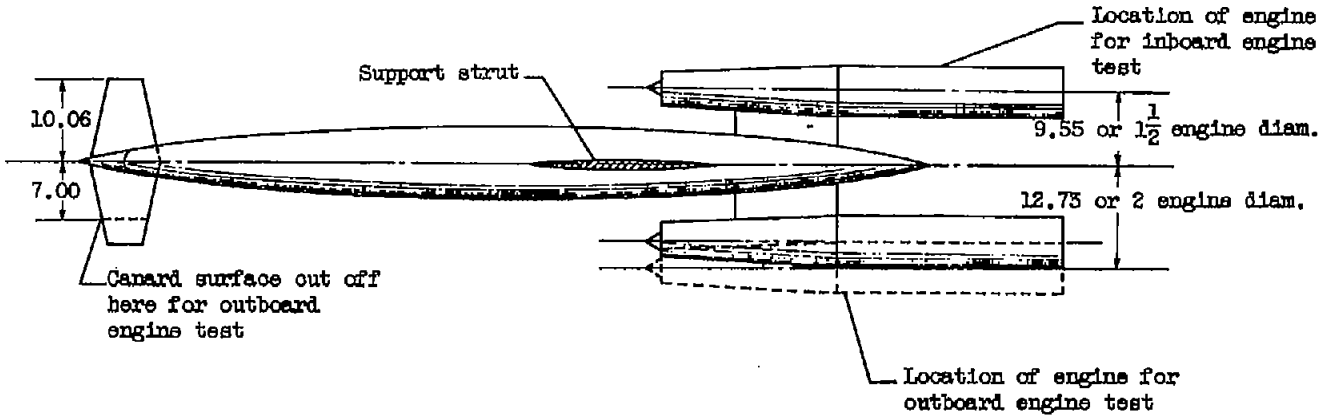

(a) Top view of model showing two engine locations.

Body defined by $d = 9\left[1-\left(1-\frac{x}{54}\right)^2\right]^{3/4}$

Body surface area, 2195 sq in.

Body volume, 4050 cu in.

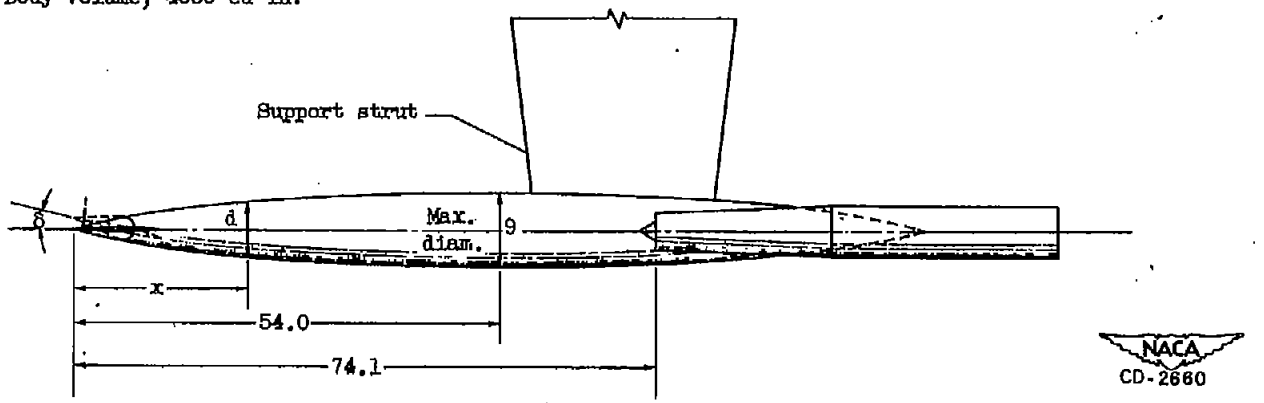

(b) Side view of model.

Figure 1. - Sketch of model showing principal geometric features. (All dimensions in inches.)

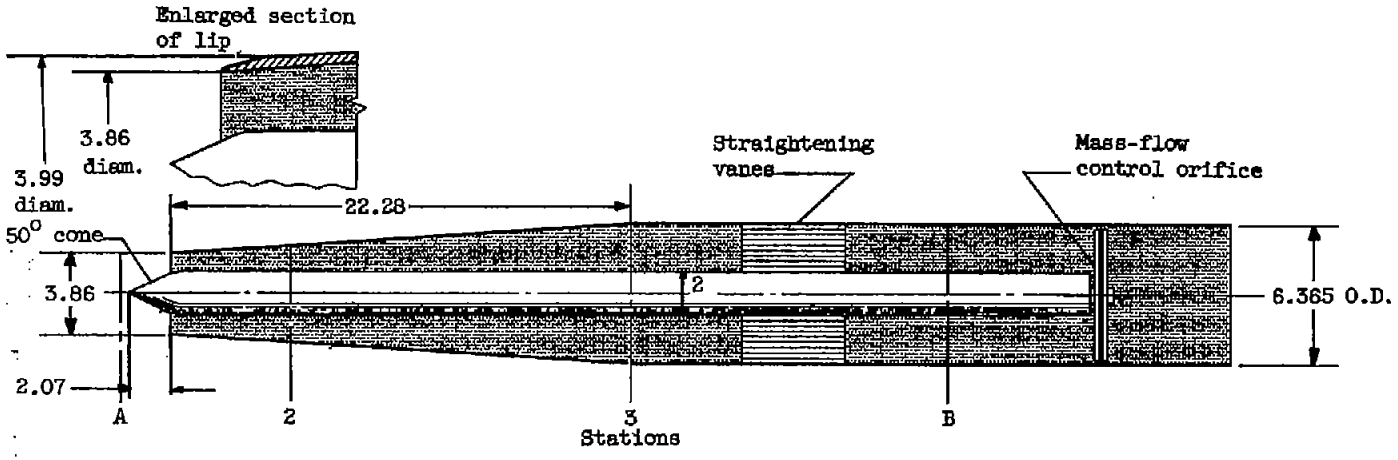

(a) Engine with original diffuser.

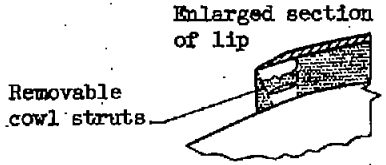

Coordinates of modified diffuser

x	0	0.15	0.40	0.65	1.15	1.65	2.15	2.34	3.15	4.15	6.90	7.65	9.65	11.06
R	1.50	1.54	1.60	1.66	1.74	1.79	1.84	1.85	←	Straight taper			→	2.48
r	0.86	0.93	1.03	1.13	1.26	1.33	1.38	1.40	1.46	1.51	1.56	1.54	1.43	1.31

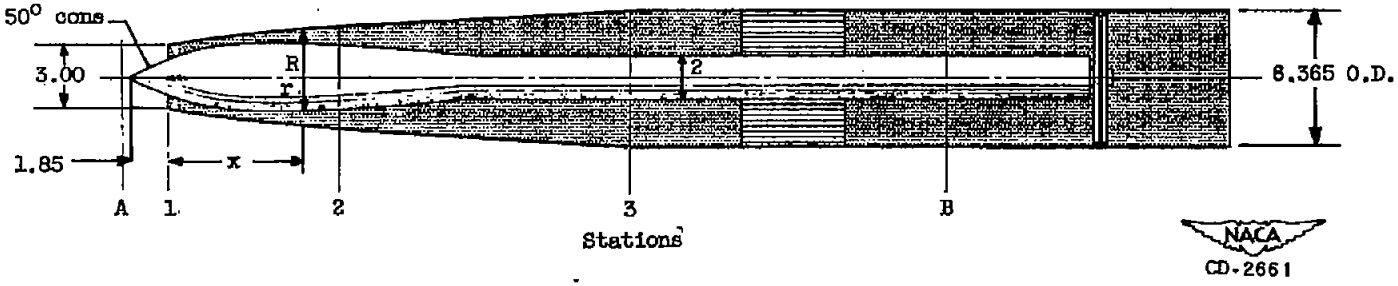

(b) Engine with modified diffuser.

Figure 2. - Sketch of ram-jet engine with two diffusers. (All dimensions in inches.)

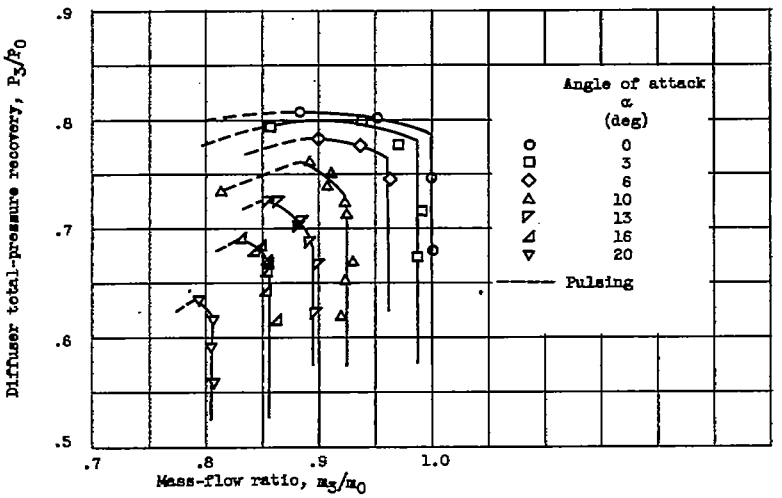

Figure 3. - Variation of total-pressure recovery with mass-flow ratio for engine alone at several angles of attack.

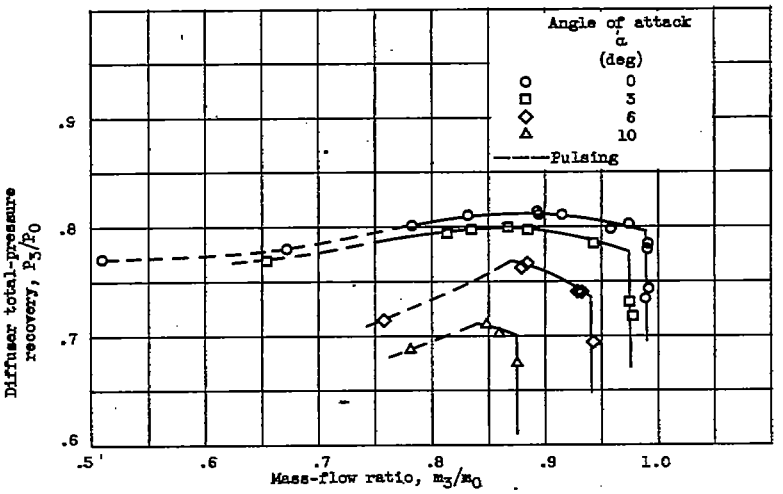

Figure 4. - Variation of total-pressure recovery with mass-flow ratio for engine-body configuration (inboard-engine location) at several angles of attack.

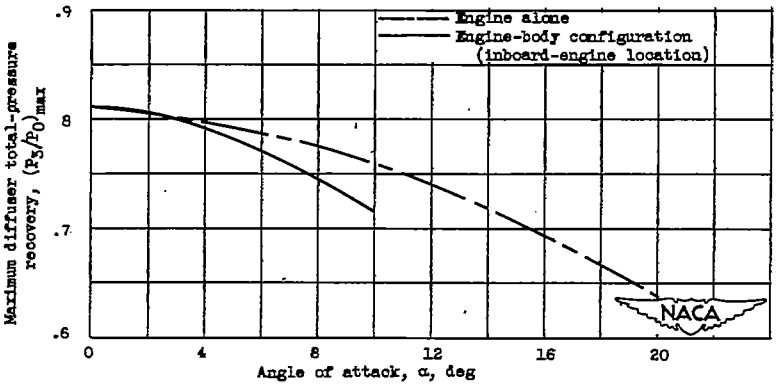

Figure 5. - Variation of maximum total-pressure recovery with angle of attack for two configurations.

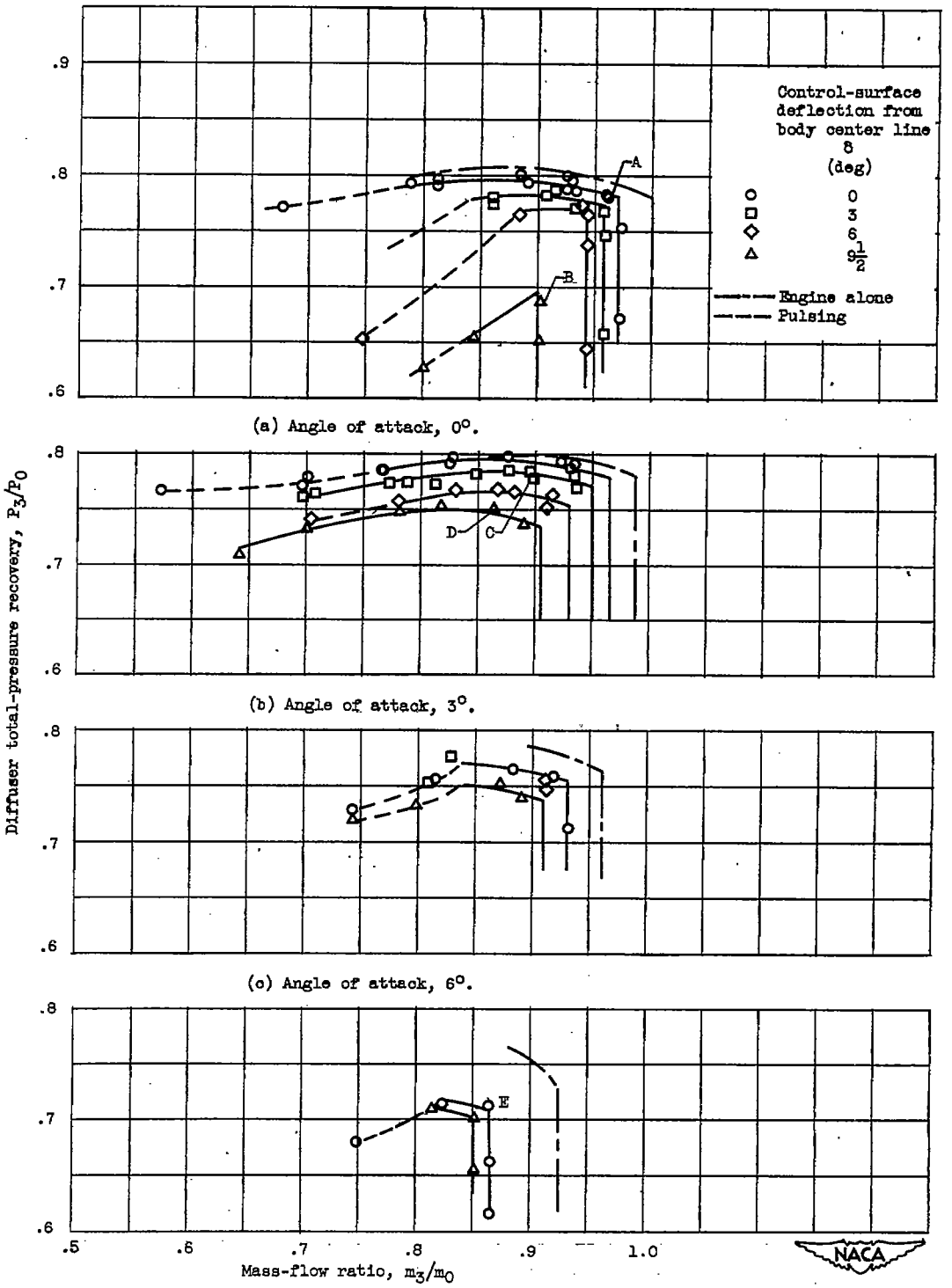

Figure 6. - Variation of total-pressure recovery with mass-flow ratio for engine-body - control-surface configuration (inboard-engine location) at several angles of attack.

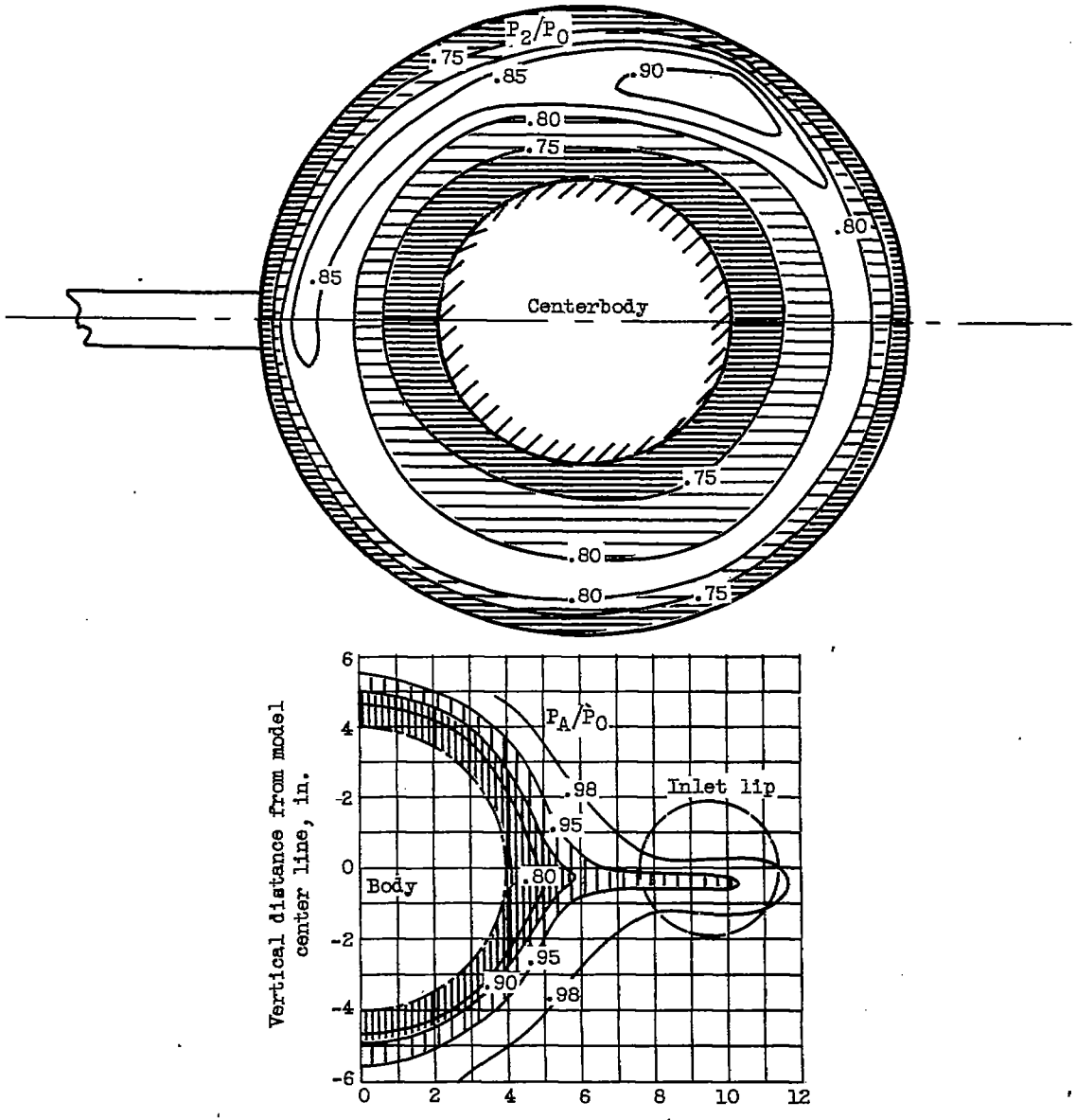

(a) Point A on figure 6. Angle of attack, 0°; control-surface deflection, 0°.

Figure 7. - Total-pressure-recovery contours at station 2 and flow survey at inlet for model with inboard-engine location at several model angles of attack and control-surface deflections.

[redacted]

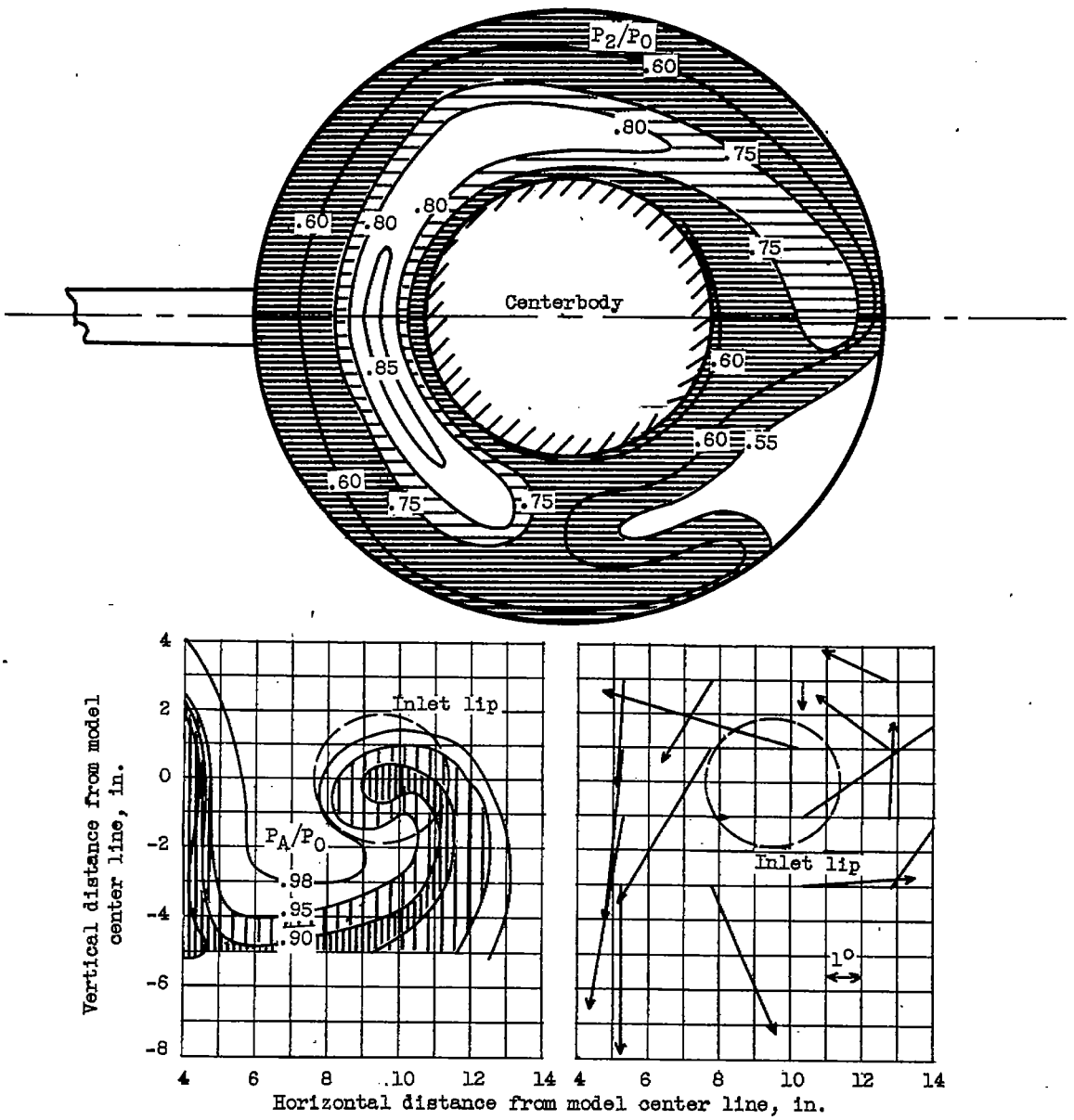

(b) Point B on figure 6. Angle of attack, 0°; control-surface deflection, $9\frac{1}{2}^\circ$.

Figure 7. - Continued. Total-pressure-recovery contours at station 2 and flow survey at inlet for model with inboard-engine location at several model angles of attack and control-surface deflections.

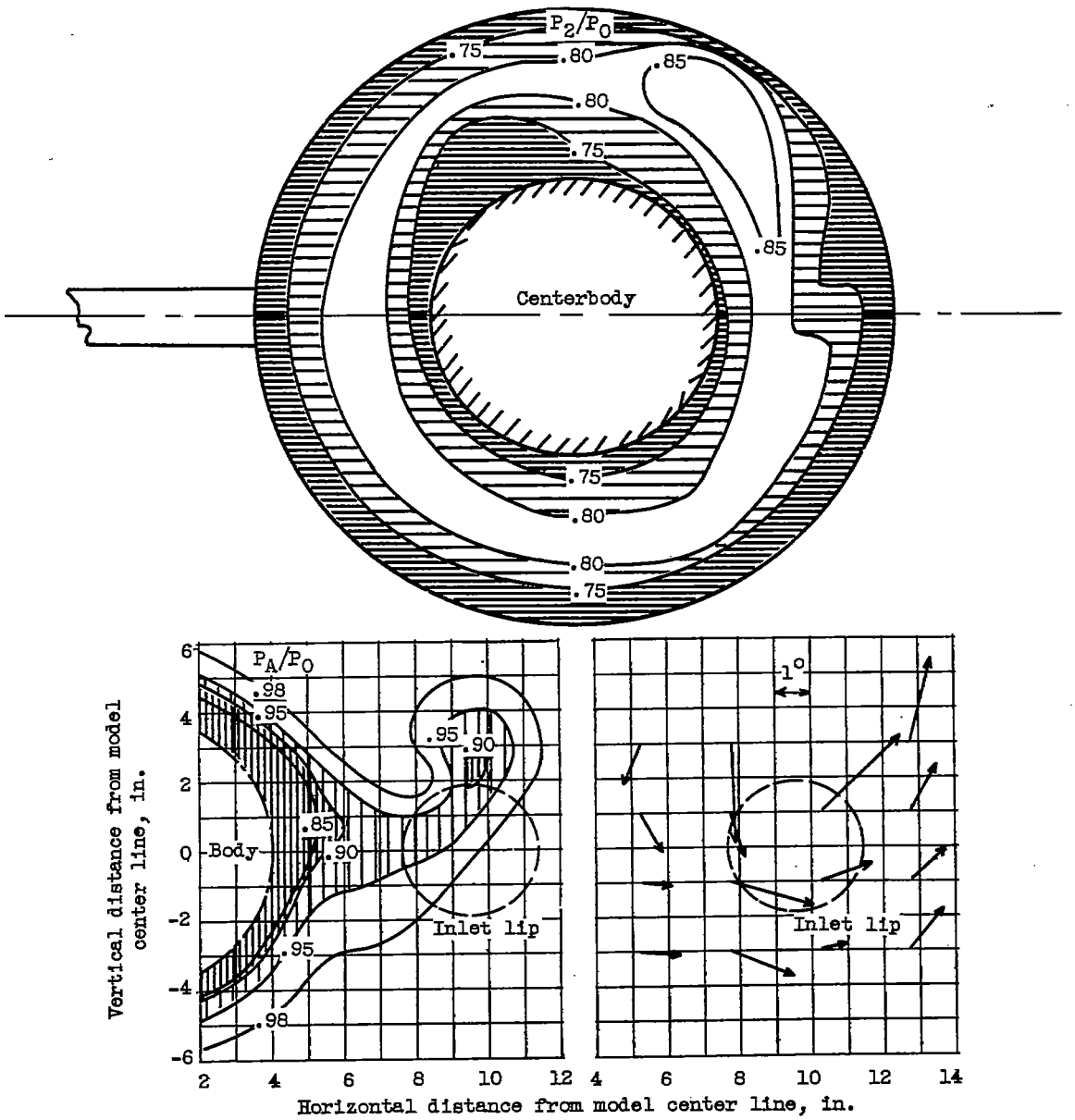

(c) Point C on figure 6. Angle of attack, 3°; control-surface deflection, 3°.

Figure 7. - Continued. Total-pressure-recovery contours at station 2 and flow survey at inlet for model with inboard-engine location at several model angles of attack and control-surface deflections.

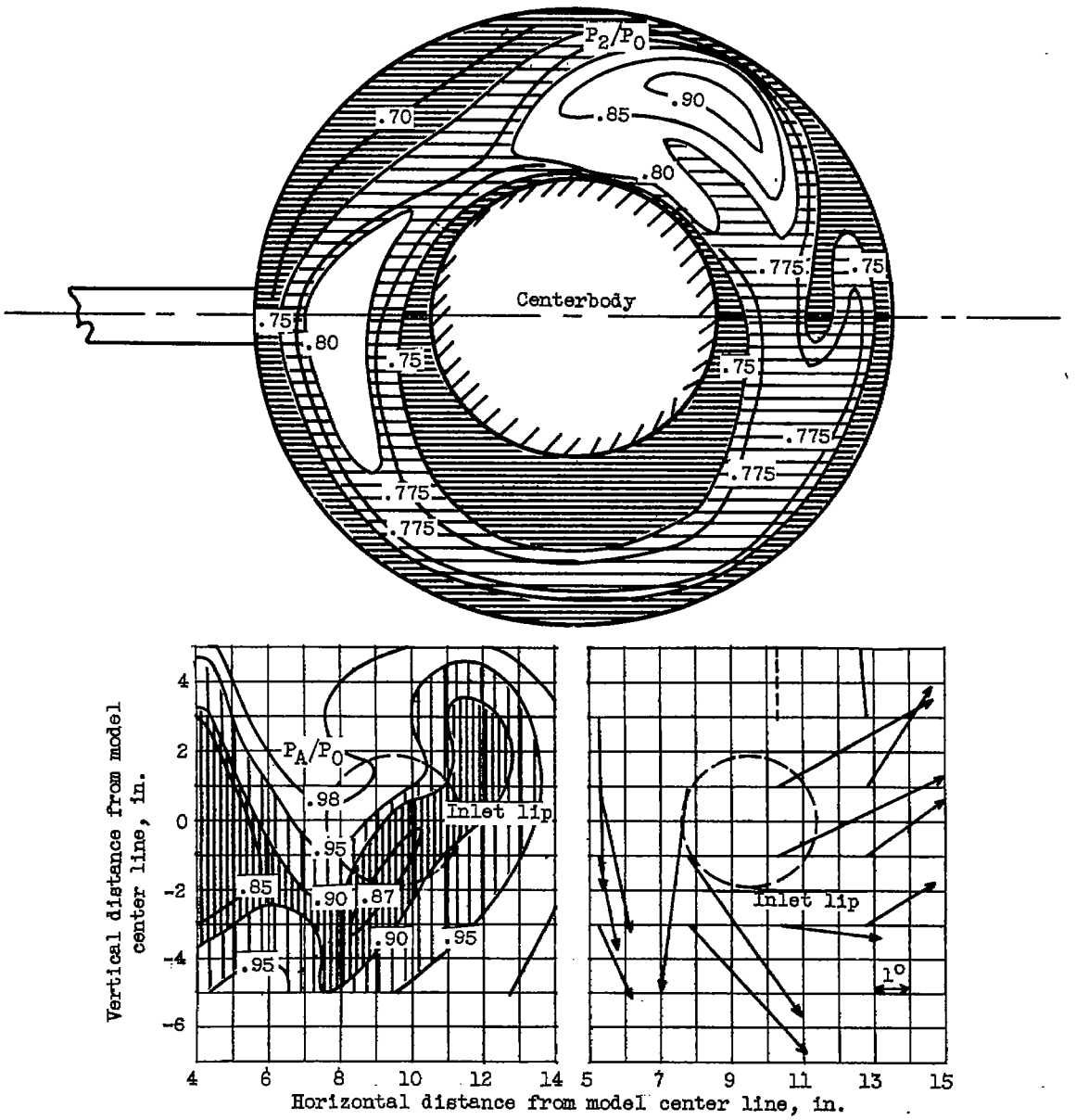

(d) Point D on figure 6. Angle of attack, 3°; control-surface deflection, $9\frac{1}{2}°$.

Figure 7. - Continued. Total-pressure-recovery contours at station 2 and flow survey at inlet for model with inboard-engine location at several model angles of attack and control-surface deflections.

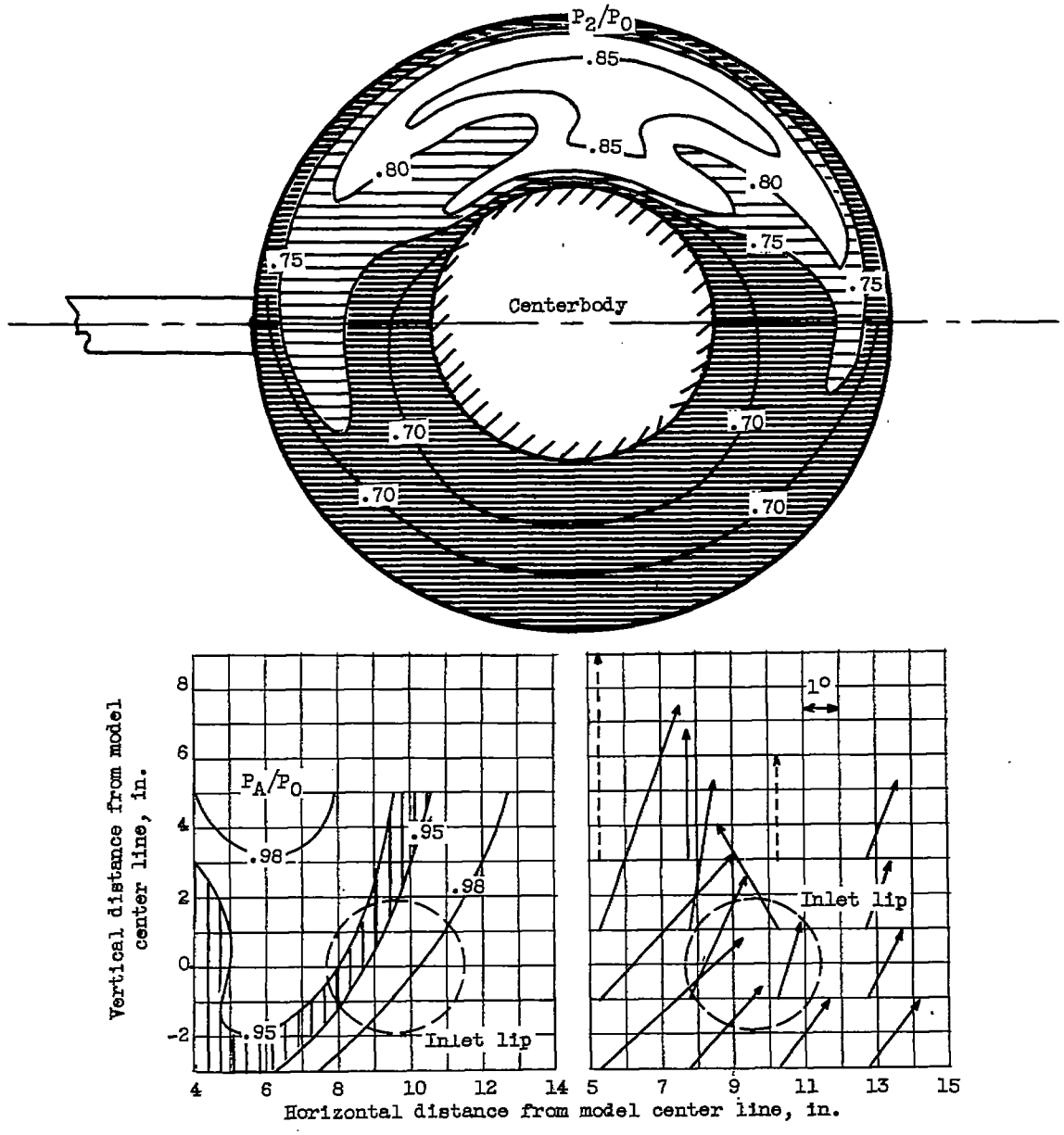

(e) Point E on figure 6. Angle of attack, 10°; control-surface deflection, 0°.

Figure 7. - Concluded. Total-pressure-recovery contours at station 2 and flow survey at inlet for model with inboard-engine location at several model angles of attack and control-surface deflections.

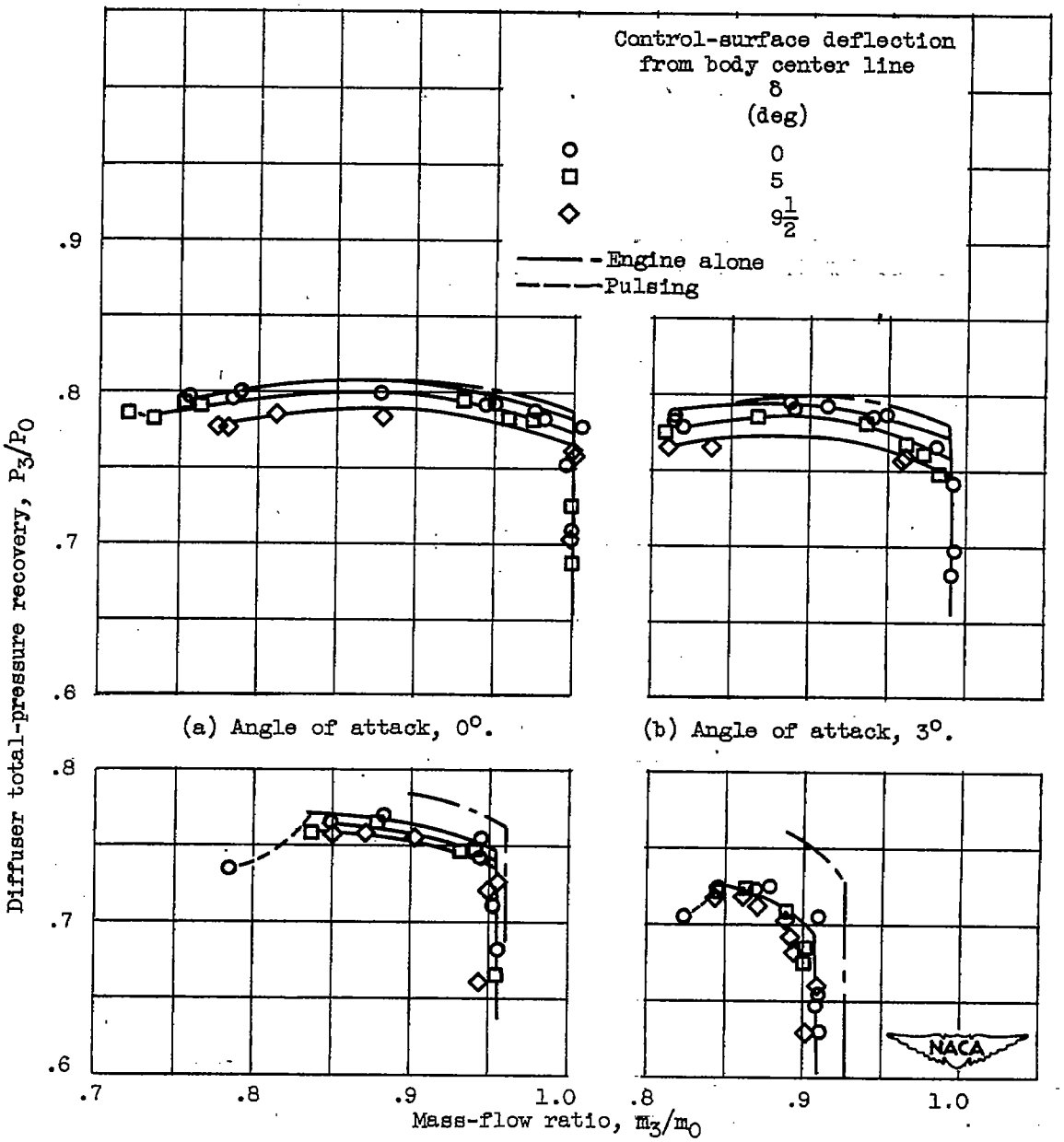

(a) Angle of attack, 0°. (b) Angle of attack, 3°.

(c) Angle of attack, 6°. (d) Angle of attack, 10°.

Figure 8. - Variation of total-pressure recovery with mass-flow ratio for engine-body - control-surface configuration (outboard-engine location) at several angles of attack.

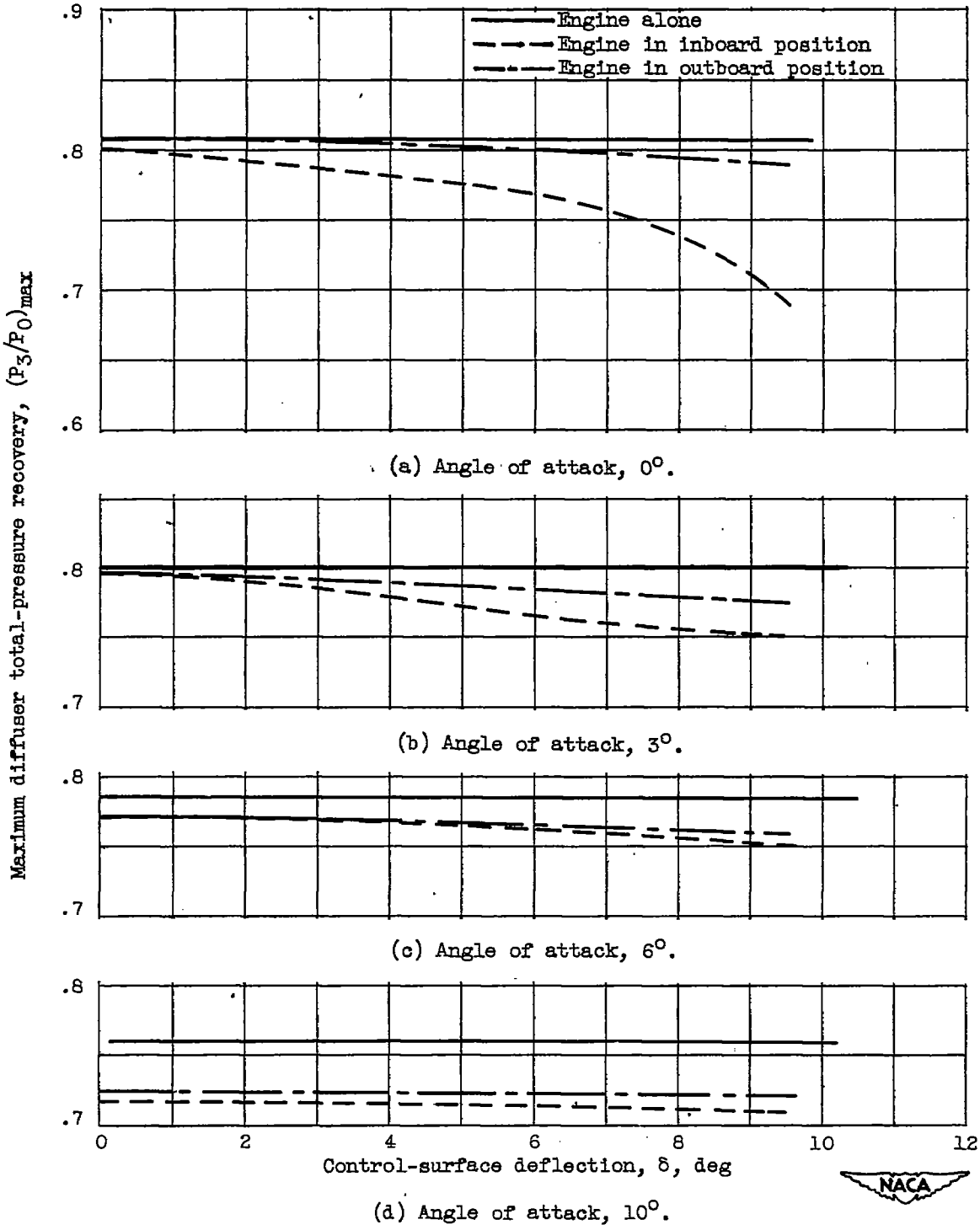

Figure 9. - Variation of maximum total-pressure recovery with control-surface deflection for two configurations at several angles of attack.

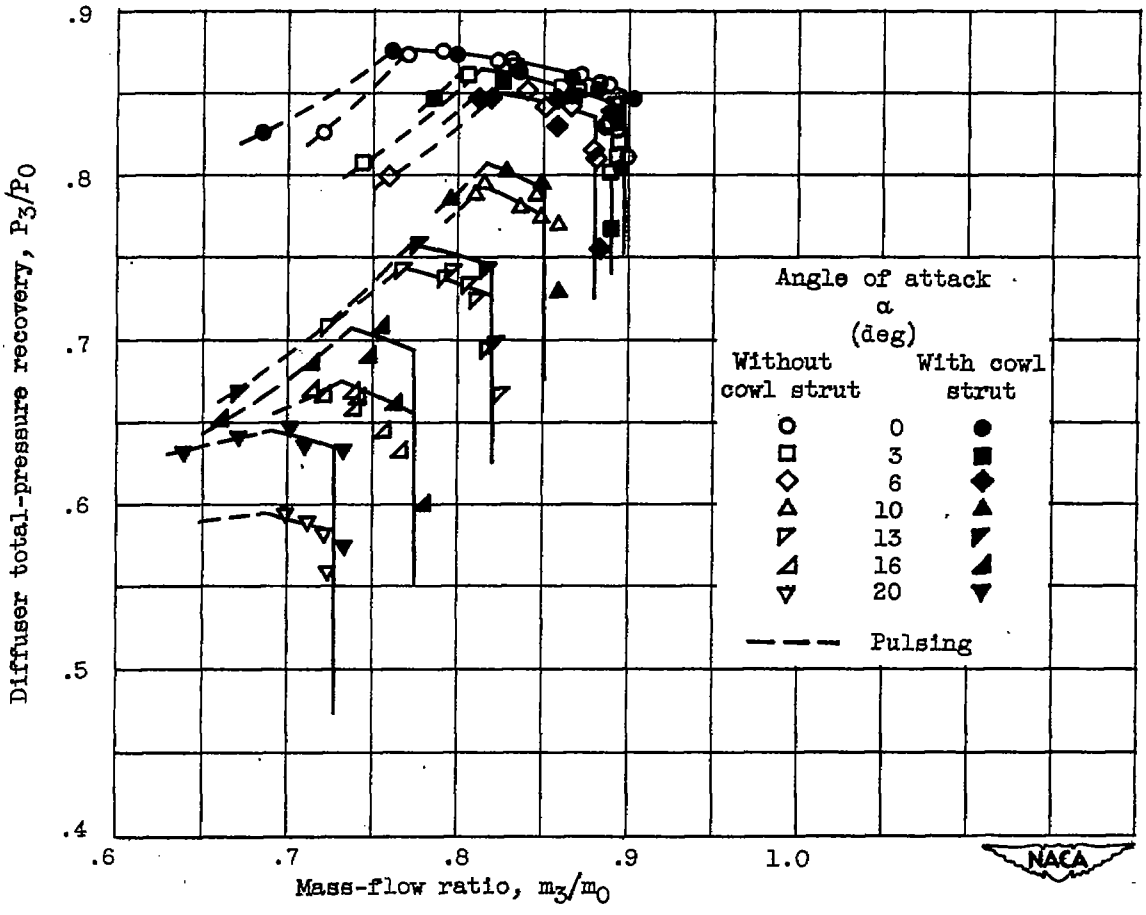

Figure 10. - Variation of total-pressure recovery with mass-flow ratio for modified engine alone with and without inlet cowl struts at several angles of attack.

[redacted]

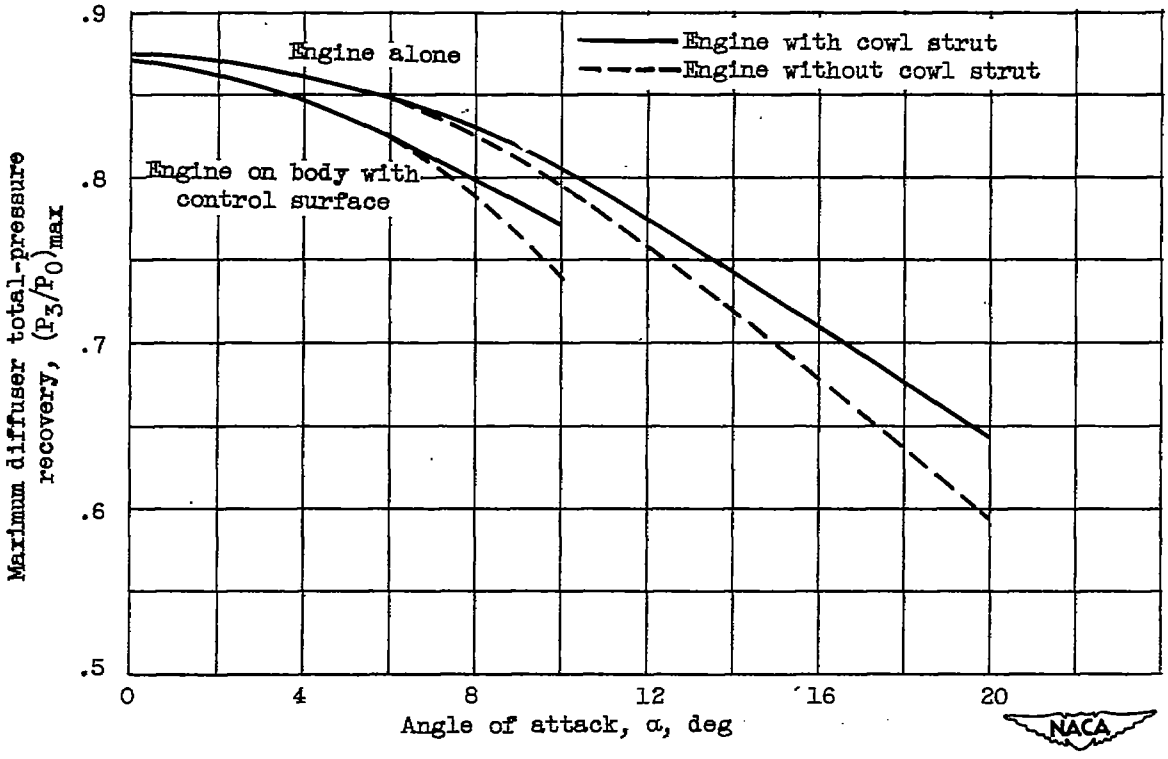

Figure 11. - Variation of maximum total-pressure recovery with angle of attack for modified engine alone and in outboard-engine location on body.

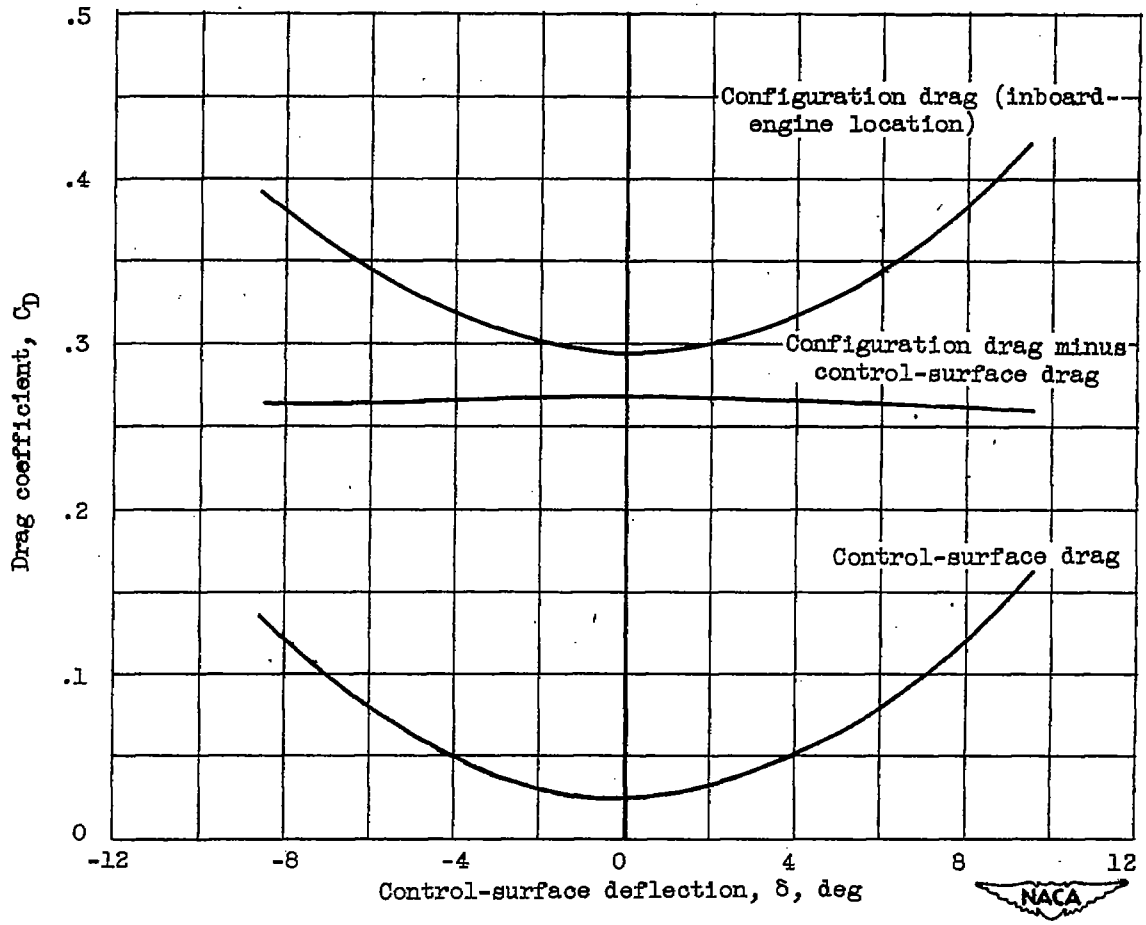

Figure 12. - Variation of configuration-drag minus control-surface-drag coefficients (including interference-drag coefficient) with control-surface deflection for an angle of attack of 0°.

NACA-Langley - 8-12-52 - 300